XXVII Congresso Nacional de Estudantes de Engenharia Mecânica
08 a 12 de fevereiro de 2021, Curitiba, PR, Brasil

MODELING AND NUMERICAL SIMULATION OF A DRY FRICTION DAMPER BASED ON A BRAKE PAD DRIVEN BY A ROD ARM APPLIED TO A SINGLE-STORY STRUCTURE

Rafael Araújo Cerqueira, rafael.cerqueira@ufba.br[1]
Marco Túlio Santana Alves, marco.alves@ufba.br[1]

[1]Universidade Federal da Bahia, Escola Politécnica, Departamento de Engenharia Mecânica, Rua Prof. Aristides Novis, 2, Federação, CEP. 40.210-630, Salvador-BA-Brazil,

Abstract. *This article presents a simple procedure for predicting time-domain vibrational behaviors of a single-story structure equiped with dry friction damper. This damper is composed by a diagonal rod arm whose its pivot is connected to platform and a brake pad is attached at the free end. The model is obtained from Newtonian mechanics considering the Coulomb damping to govern the dissipative force action. The nonlinear differential equation of motion is solved numerically by using the Runge-Kutta's method built in Scilab. Both free and forced vibration responses were simulated, considering several values for the rod arm angle and coefficient of friction. The results, for both vibration amplitude and dissipated power, revealed that for higher values of rod arm angle and coefficient of friction the performance of dry friction damper increase significantly.*

Keywords: *dry friction damper, Coulomb damping, passive vibration control, numerical methods, single-story structure*

1. INTRODUCTION

According to Belash (2015), currently, due to the increased requirement to control the vibration amplitude of structures (especially large ones), researchers have investigated more and more the benefits of dry-friction as a solution for this problem. Based on Ferri (1995), the friction damping will continue to play an important role in many mechanical and structural systems, since it is one of several forms of passive control (with no external energy required).

A dry-friction tuned mass damper (TMD) composed by two devices was proposed by Inaudi and Kelly (1995), where the system is nonlinear with hysteresis behavior by adopting the small displacements hypothesis. Ricciardelli and Vickery (1999) studied a single degree of freedom system response subject to a harmonic excitation in which a dynamic vibration absorber with linear stiffness and dry-friction is considered. Krenk (2005) designed a dry-friction TMD, pointing out important parameters like the benefit of choosing a low mass ratio. An extended study about the TMD parameters optimization was carried out by Bakre and Jangid (2007), where they developed explicit expressions with a good agreement with the numerical research technique. Finally, Lin *et al.* (2010) used a hybrid vibration control system adapted a dry-friction TMD, to vary the applied force, besides they also evaluated multiple TMD performances in a seismic structure.

In this context, this paper is devoted to simulate a single-story structure equiped with a dry-friction damper composed by a diagonal rod arm and a brake pad attached to the rod arm free end. Thus, the main intention of this work is investigate numerically the damper performance (free and forced responses) for several configurations in terms of rod arm angle and coefficient of friction between brake pad and floor surfaces.

Thus, the structure for this contribution is presented. Besides this introductory section, the basics of Coulomb damping, the single-story structure modeling with its properties, the results in terms of vibration amplitude and dissipated power and, finally, the concluding remarks are then presented.

2. THEORETICAL BACKGROUND

2.1 Coulomb damping or Dry-Friction damping

Coulomb damping is the damping that occurs due to dry friction when two surfaces slide against one another. Coulomb damping can be the result of a mass sliding on a dry surface, axle friction in a journal bearing, belt friction, or rolling resistance. The case of a mass sliding on a dry surface is analyzed here, but the qualitative results apply to all forms of Coulomb damping. As the mass (m) of "Fig. 1" slides on a dry surface, a friction force that resists the motion develops between the mass and the surface. Coulomb's law states that the friction force is proportional to the normal force (N) developed between the mass and the surface. The constant of proportionality, is called the kinetic coefficient of friction

(μ). Since the friction force always resists the motion, its direction depends on the sign of the velocity ($\dot{x}$) (Kelly, 2012). Details regarding to the tribological phenomena that take place between the sliding surfaces can be found in Dahl (1976) and in textbooks (Bhushan, 2002; Hutchings and Shipway, 2017) since this is not treated in this article. According to Inman (2013), Coulomb damping is characterized by the relation

$$f_c = F_c(\dot{x}) = \begin{cases} -\mu N & \text{if } \dot{x} > 0 \\ 0 & \text{if } \dot{x} = 0 \\ \mu N & \text{if } \dot{x} < 0 \end{cases} \tag{1}$$

where f_c is the dissipative force (always acts in a direction opposite to the direction of velocity).

Consider a single-degree-of-freedom system with dry friction (free vibration) as shown in "Fig. 1".

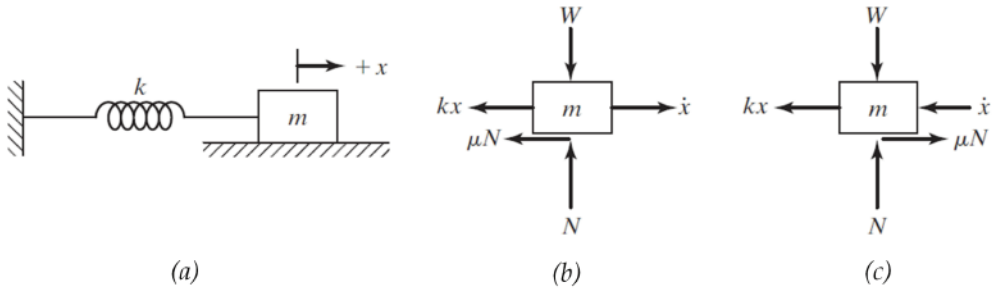

Figure 1. Spring-mass system with Coulomb damping (adapted from Rao (2010))

Based on "Fig. 1(a)" and "Fig. 1(b)" the equations of motion are written for the mass moving to the right and to the left, respectively. However, it is possible to merge them into a unique equation by using the approach in (1), as following

$$m\ddot{x} + \mu N \,\mathrm{sgn}\,(\dot{x}) + kx = 0 \tag{2}$$

where m and k are the mass and stiffness, respectively; sgn is a *signum* function that play the role to identify the velocity $\dot{x}$ over the time. Based on Inman (2013), this is a typical nonlinear system whose the idea of a single equilibrium position is lost. Thus, a continuous region of equilibrium position exists. As the "Eq. (2)" is a nonlinear differential equation, a simple analytical solution does not exist such way that numerical methods can be used to solve it (Rao, 2010). By the way, in case of forced vibration a excitation force $F(t)$ will appear in the right-hand side of "Eq. (2)".

3. METHODOLOGY

The single-story structure designed by the authors basically consists of a platform supported by four elastic columns and the dry friction damper is made up of a brake pad connected to the platform by a pivoted rod at the ends, as shown in "Fig. 2" It is a single DOF system in such way that the motion takes place strictly along horizontal direction (x-axis).

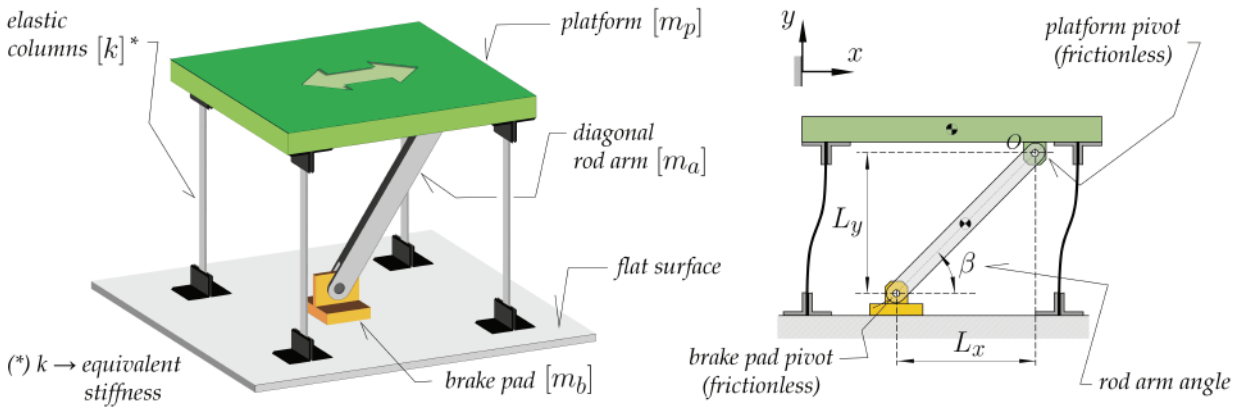

Figure 2. Schematics of single-story structure connected to dry friction damper

The assumptions for this work are following summarized: small displacements; the motion only takes place along

horizontal direction; both pivots are frictionless; all elastic columns works in linear region (linear stiffness); the rod arm is assumed as a homogeneous rigid bar; no viscous damping; xy-plane is the symmetry plane of the system.

3.1 System modeling based on Newtonian mechanics

To modeling systems damped by dry friction action it is necessary split the motion into two half-cycles, as follows: system moving to the right ($\dot{x} > 0$) and moving to the left ($\dot{x} < 0$) as represented by the free body diagrams (FBDs) in "Fig. 3".

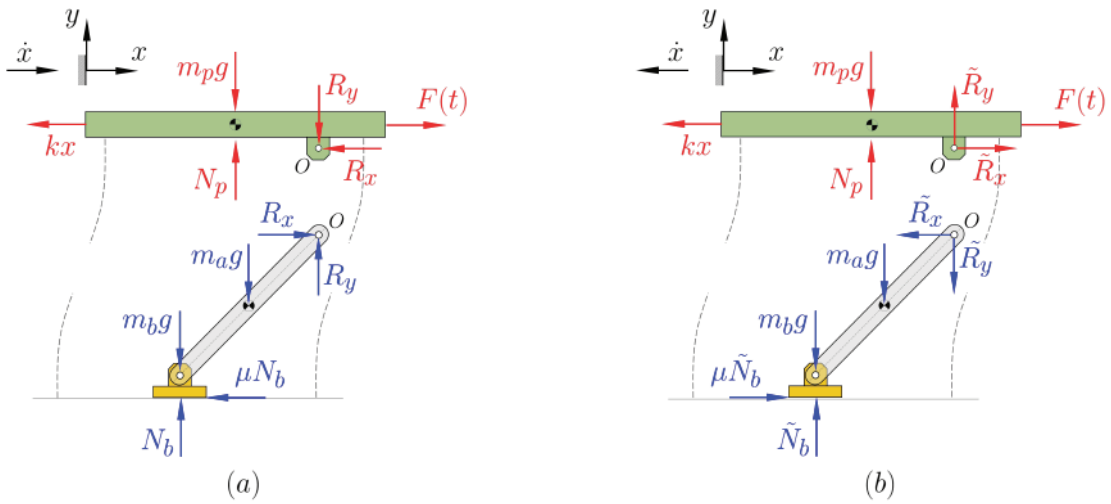

Figure 3. Free body diagrams (FBDs): (a) half-cycle system moving to the right; (b) half-cycle system moving to the left

To start modeling, the damper is isolated from the platform. From the point of view of rotational motion the damper is assumed static and both pivots are frictionless. For this reason it is possible apply static equilibrium condition for the moments summation to the damper (rod arm and brake pad) about the point 'O'. Accordingly to this condition, the intention is calulate the normal force onto the brake pad. Thus, for the first half-cycle (see"Fig. 3(a)"), it can be concluded that the moment (clockwise sense) due to the friction force ($f_c = \mu N_b$) about point 'O' transfer no force to the platform along vertical direction. Thus, as the point 'O' is assumed frictionless and there is no constrain to the rod arm rotates in clockwise sense, as a result it is as if the block is at rest. Then, the friction force is neglected before applying equilibrium condition, as following performed:

$$cw(+)\sum M_O = 0 \Rightarrow N_b L_x - m_b g L_x - m_a g(L_x/2) = 0 \Rightarrow N_b = \left(m_b + \frac{m_a}{2}\right) g \tag{3}$$

consequently the normal force N_b is not affected whenever $\dot{x} > 0$.

Nevertheless, for the other half-cycle (see"Fig. 3(b)"), the moment due to the friction force ($\tilde{f} = \mu\tilde{N}_b$) about point 'O' is in counterclockwise sense. Therefore, in this case the rod arm is constrained since it cannot rotate freely. Thereby, the static equilibrium condition have to be applied to the damper (considering the forces in blue in FBD), as follows:

$$cw(+)\sum M_O = 0 \Rightarrow \tilde{N}_b L_x - m_b g L_x - m_a g(L_x/2) - \mu\tilde{N}_b L_y = 0 \Rightarrow \tilde{N}_b = \left(m_b + \frac{m_a}{2}\right) g \left(\frac{L_x}{L_x - \mu L_y}\right) \tag{4}$$

where $\tilde{N}_b$ is the normal reaction force on brake pad when the system moves to the left; L_x and L_y are the horizontal and vertical distances between both pivots, respectively. Based on the geometry related to the system, it is clear that $\tan\beta = L_y/L_x$. Thus, from "Eq. (4)", N_b can be rearranged, as follows

$$\tilde{N}_b = \left(m_b + \frac{m_a}{2}\right) g \left(\frac{1}{1 - \mu\tan\beta}\right) \tag{5}$$

From "Eq. (5)" an amplification factor $\tilde{\gamma}$ can be extracted and must be used whenever ($\dot{x} < 0$). It can be expressed as

$$\tilde{\gamma} = \frac{1}{1 - \mu\tan\beta} \tag{6}$$

From now on, the dynamics is considering by applying Newton's second law to both FBDs in "Fig. 3". Firstly for the half-cycle related to the motion to the right, where the focus is directed to the platform in "Fig. 3(a)" (forces in red), as following performed

$$\rightarrow (+) \sum F_x = (m_b + m_a)\ddot{x} \Rightarrow R_x - \mu N_b = (m_b + m_a)\ddot{x} \Rightarrow R_x = (m_b + m_a)\ddot{x} + \mu N_b \tag{7}$$

Now, in this turn the second law is applied to the damper (rod arm and brake pad) to obtain the equation of motion for the system moving to the right ($\dot{x} > 0$)

$$\rightarrow (+) \sum F_x = m_p\ddot{x} \Rightarrow -R_x - kx + F(t) = m_p\ddot{x} \Rightarrow m\ddot{x} + \mu N_b + kx = F(t) \tag{8}$$

where $m = m_p + m_a + m_b$

Analogously, the same procedure is used for the platform and the damper as diagrammatized in "Fig. 3(b)", where the system moves to the left. Hence,

$$\rightarrow (+) \sum F_x = (m_b + m_a)\ddot{x} \Rightarrow -\tilde{R}_x + \mu\tilde{N}_b = (m_b + m_a)\ddot{x} \Rightarrow \tilde{R}_x = -(m_b + m_a)\ddot{x} + \mu\tilde{N}_b \tag{9}$$

Therefore, the equation of motion for the system moving to the left to obtain the equation of motion for the system moving to the right ($\dot{x} < 0$) is obtained as follows

$$\rightarrow (+) \sum F_x = m_p\ddot{x} \Rightarrow \tilde{R}_x - kx + F(t) = m_p\ddot{x} \Rightarrow m\ddot{x} - \mu\tilde{N}_b + kx = F(t) \tag{10}$$

Since both "Eq. (8)" and "Eq. (10)" are obtained, they can be summarized in their final forms

$$m\ddot{x} + \mu\left(m_b + \frac{m_a}{2}\right)g + kx = F(t) \rightarrow \dot{x} > 0 \tag{11}$$

$$m\ddot{x} + kx = F(t) \rightarrow \dot{x} = 0 \tag{12}$$

$$m\ddot{x} - \mu\tilde{\gamma}\left(m_b + \frac{m_a}{2}\right)g + kx = F(t) \rightarrow \dot{x} < 0 \tag{13}$$

Thereby, "Eq. (11)", "Eq. (10)" and "Eq. (8)" and "Eq. (11)" will be solved using the strategy established in the next section.

3.2 Strategy for numerical simulation

This section is dedicated to present the strategy to be used in order to generate the results. All numeric values to be assigned to each parameter in the model represented by "Eq. (11)" are shown in "Tab. 1". The reader can note that will be simulated four different coefficients of friction and two rod arm angles.

Table 1. Main system properties (single-story + damper)

platform mass	rod arm mass	brake pad mass	equivalent stiffness	rod arm angle		coefficient of friction			
$m_p\ [kg]$	$m_a\ [kg]$	$m_b\ [kg]$	$k\ [N/m]$	$\beta\ [deg]$		μ			
2.5	0.1	0.4	5×10^3	30	60	0.0	0.1	0.2	0.3

Firstly, the system will be simulated for free vibration response and the initial conditions for this case is $x(0) = 5\ mm$ and $\dot{x}(0) = 0\ m/s$. Since the natural frequency for this system is $\omega_n \approx 6.5\ [Hz]$, it was chosen a excitation frequency $\omega = 6.0\ Hz$ to avoid the response divergence (instability) despite of beating phenomenon, whose response is stable. From this scenario, it will be performed a forced responses due to a harmonic excitation given by $F(t) = F_0 \sin \omega t$ where its amplitude is $F_0 = 5\ N$ and the time simulation is $30\ s$.

The approach used to solve the equation of motion expressed by "Eq. (12)" was proposed by Sallet (2004) where basically some parameters was adapted to apply the function "ODE" in Scilab to solve ordinary differential equations with no risk for numerical divergence during the processing of computational code.

4. RESULTS AND DISCUSSIONS

This section is dedicated to present all results based on the strategy designed in the previous section

4.1 Correction factors of normal reaction force on brake pad

"Figure 4" presents the iscocurves related to amplification factor $\tilde{\gamma}$) from a swept on parameters μ (coefficient of friction) and β (diagonal rod arm angle) by using "Eq. (7)".

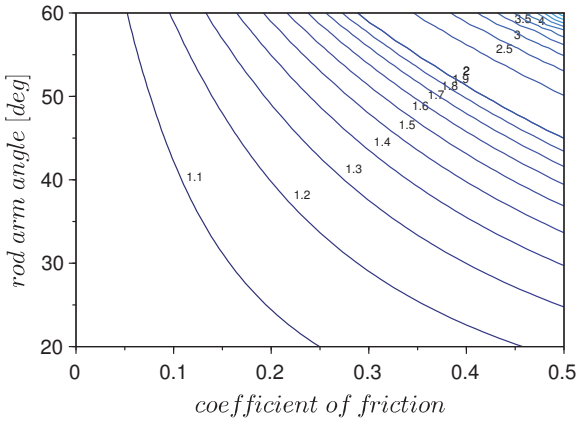

Figure 4. Isocurves of amplification factor $\tilde{\gamma}$ of normal on the brake pad

At a first glance, it is noted that for $\tilde{\gamma}$, all values are greater than unity. Since this work is dealing with a dry friction damper, it is clear that the set composed by the brake pad driven by a rod arm exhibits self-energizing behavior whenever the system moves to the left (Norton, 1997). In other words, in this condition the damper amplifies its energy dissipation capacity. In the same way, depending on the combination of parameters $\tilde{\gamma}$ and β the damper may exhibit self-locking behavior, not investigated in this contribution.

4.2 Single-story structure - free response

The results shown in "Fig. 5" are related to the system free response considering the rod arm angles $\beta = 30\ deg$ and $\beta = 60\ deg$.

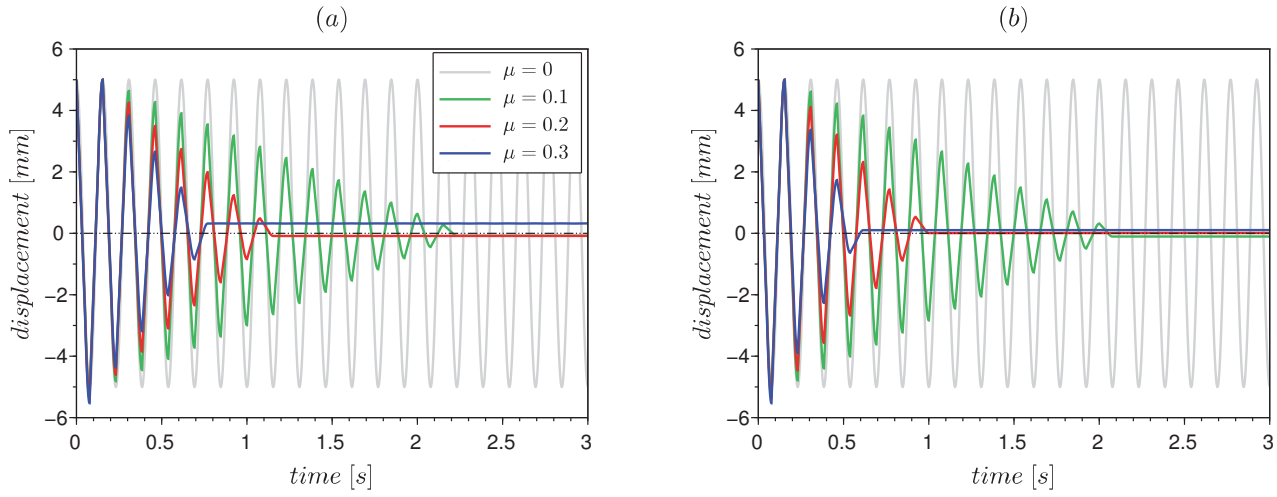

Figure 5. Platform displacement time history (free response): (a) rod arm angle $\beta = 30\ deg$; (b) rod arm angle $\beta = 60\ deg$

From an overall perspective, the responses presented for both graphs revealed that the larger coefficient of friction the more rapidly is the decay, regardless the rod arm angle. Other key finding is the confirmation of the typical linear decay for system damped due to dry friction. Besides, it can be noted that the system not necessarily comes back to the original equilibrium position. All these points can be found more detailed in mechanical vibration textbooks (Thomson

and Dahleh, 2005; Rao, 2010). Additional comments will be made later.

4.3 Single-story structure - forced response due to sinusoidal input

"Figure 6" present the results related to forced response considering two rod arm angles, as follows: $\beta = 30\ deg$ and $\beta = 60\ deg$.

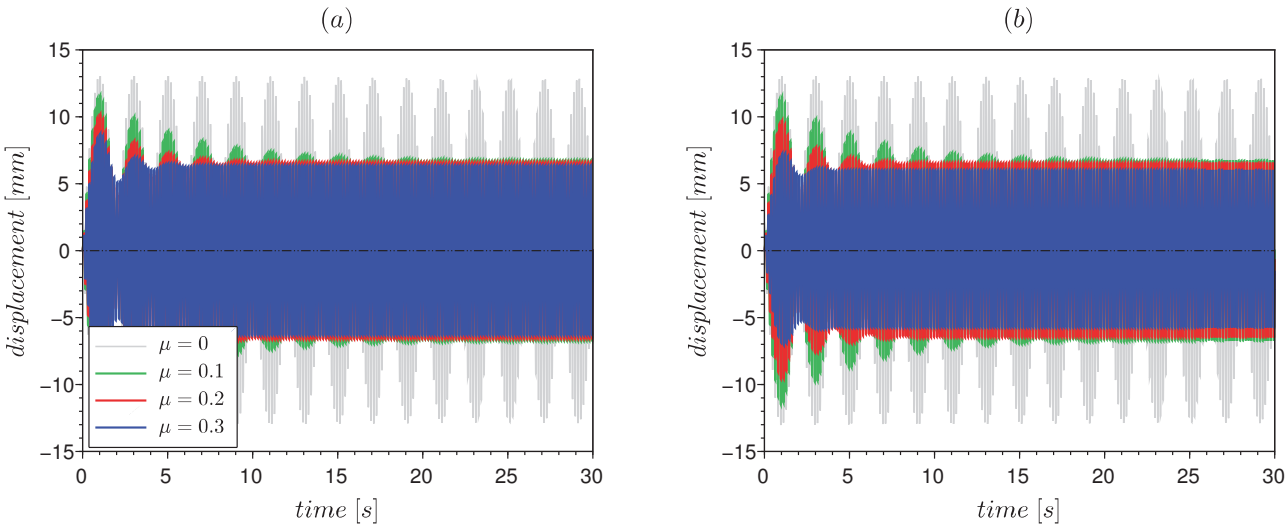

Figure 6. Platform displacement time history (forced response - sine wave): (a) rod arm angle $\beta = 30\ deg$; (b) rod arm angle $\beta = 60\ deg$

At a first sight, the reader can observe that for both graphs the overall behavior is quite similar, however the reponse stabilize earlier for a larger rod arm angle besides the reduction level slightly smaller, as can be checked in “Fig. 6(b)”. Just for reference, it was simulated the system with no friction (light gray curves). As there is no viscous damping, it was necessary to choose an excitation frequency close to the natural frequency in order to emphasize the amplitude vibration with no response divergence. For this reason a harmless side effect, considering the purpose of this work, takes place: the beating phenomenon.

Another aspect investigated relies on the dissipated power. “Figure 7” shows the dissipated power evolution over time for the same afforementioned rod arm angles. By analyzing “Fig. 7(a)” and “Fig. 7(b)”, it is concluded that the larger arm angle the larger is the amount of dissipated power.

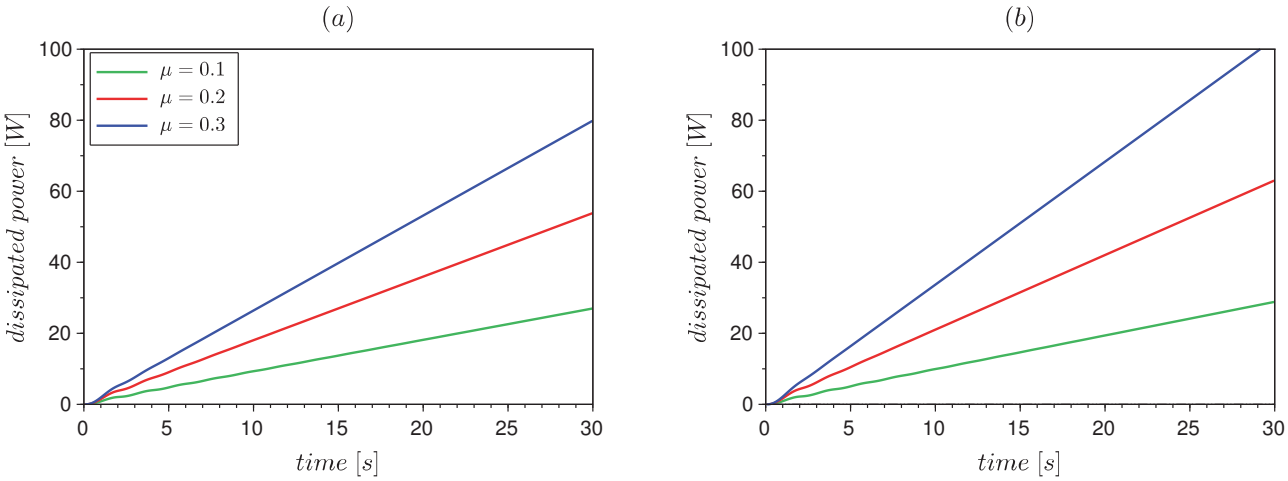

Figure 7. Dissipated power evolution (forced response): (a) rod arm angle $\beta = 30\ deg$; (b) rod arm angle $\beta = 60\ deg$

In order to integrate the analysis of the results (including free and forced responses), the “Tab. 2” was created to make this task easier. Actually, all key results were summarized within the same table to allow direct comparison among the inherent parameters. Thus, based on this strategy, it is important to define new parameters, as follows: f_c and $\bar{f}_c$ are the friction forces when the platform moves to the right and left, respectively; n_c is the number of cycles; t_e is the

stabilization time; x_e is the steady-state amplitude (displacement); P_d is the dissipated power due to friction force; and δ is the amplitude reduction compared to the frictionless system. The rest of the parameters present in the table have already been previously defined in the text.

Table 2. Summary of simulated results for free and forced responses

$\beta\ [deg]$	friction force				free response		forced response			
	μ	$\tilde{\gamma}$	$f_c\ [N]$	$\tilde{f}_c\ [N]$	n_c	$t_e\ [s]$	$x_e\ [mm]$	$\delta\ [\%]$	$P_d\ [W]$	$t_e\ [s]$
30	0.1	1.06	0.44	0.47	15	2.22	6.77	47.2	27.0	30.0
	0.2	1.13	0.88	1.00	7	1.16	6.62	48.4	53.8	16.7
	0.3	1.21	1.32	1.60	5	0.79	6.37	50.4	79.8	6.9
60	0.1	1.21	0.44	0.53	13	1.85	6.76	47.3	28.8	30.0
	0.2	1.53	0.88	1.35	6	0.85	6.58	48.7	63.0	10.4
	0.3	2.08	1.32	2.76	4	0.54	6.04	53.0	102.9	4.8

By performing an overall analysis on free response results, it is clear that the larger rod arm angles the smaller the number of oscillations until the system stops. Besides, as a natural consequence, the stabilization time also decreases. Moreover, by focusing on the variation of coefficient of friction (in ascending order), the effect on number of cycles and stabilization time will be the same as afforemetioned. From the forced response perspective, the amplitude reduction δ decreases whenever both rod arm angle and coefficient of friction increase. As the expression for amplification factor $\tilde{\gamma}$ (see "Eq.(6)") is clearly nonlinear (as confirmed by the isocurves in "Fig. 4"), the reduction levels δ for $\mu = 0.1$ and $\mu = 0.2$ (despite of rod arm angle) is quite similar. However, for $\mu = 0.3$ the reduction is more significant. All mentioned reduction is related to the force friction whenever the platform moves to the left ($\tilde{\gamma}$). Consequently, the work done by the sliding frictional force over time is larger being numerically equal to dissipated power. Even the system vibrates in resonant region the damper is capable to drain vibrational energy such that the stabilization time decreases as shown in last column of "Tab. 2". It is important to recover that as the system operates in a unique frequency, the performance of damper depends on the normal amplification factor that in turn depends on damper geometry (rod arm angle β) and the pair of surfaces (coefficient of friction μ). Certainly, if higher values of angle and coefficients of friction had been tested, the performance of the damper would increase significantly, and may tend to self-locking, not investigated in this work.

5. CONCLUDING REMARKS

In order to check the potentialities for numerical integration approach proposed by Sallet (2004), a computational code was implemented to simulate the dynamic behavior of a single-story structure equiped with a dry-friction damper composed by a rod arm and a brake pad. Assuming the Coulomb's law for the friction, the results revealed a reasonable performance for both cases simulated: free and forced response (sinusoidal excitation). Therefore, the increase in passive control performance from the damper designed by the authors is directly linked to the increase in the rod arm angle and coefficient of friction values. Finally, considering all simulations carried out the reduction on amplitude vibration is up to 53%.

6. REFERENCES

Bakre, S.V. and Jangid, R.S., 2007. "Optimum parameters of tuned mass damper for damped main system". *Structural Control and Health Monitoring*, Vol. 14, No. 3, pp. 448–470.

Belash, T., 2015. "Dry friction dampers in quake-proof structures of buildings". *Procedia Engineering*, Vol. 117, pp. 397 – 403.

Bhushan, B., 2002. *Introduction to Tribology*. Wiley, 1st edition.

Dahl, P.R., 1976. "Solid friction damping of mechanical vibrations". *AIAA Journal*, Vol. 14, No. 12, pp. 1675–1682.

Ferri, A.A., 1995. "Friction damping and isolation systems". *Journal of Vibration and Acoustics*, Vol. 117, pp. 196 – 206.

Hutchings, I. and Shipway, P., 2017. *Tribology: Friction and Wear of Engineering Materials*. Butterworth-Heinemann, 2nd edition.

Inaudi, J.A. and Kelly, J.M., 1995. "Mass damper using friction-dissipating devices". *Journal of Engineering Mechanics*, Vol. 121, No. 1, pp. 142–149.

Inman, D.J., 2013. *Engineering Vibrations*. Pearson, 4th edition.

Kelly, S.G., 2012. *Mechanical Vibrations - Theory and Applications*. Cengage Learning, 1st edition.

Krenk, S., 2005. "Frequency Analysis of the Tuned Mass Damper". *Journal of Applied Mechanics*, Vol. 72, No. 6, pp.

936–942.

Lin, C.C., Lu, L.Y., Lin, G.L. and Yang, T.W., 2010. "Vibration control of seismic structures using semi-active friction multiple tuned mass dampers". *Engineering Structures*, Vol. 32, No. 10, pp. 3404 – 3417.

Norton, R.L., 1997. *Machine Design - An Integrated Approach*. Prentice Hall, New Jersey, 1st edition.

Rao, S., 2010. *Mechanical vibrations*. Prentice Hall, 5th edition.

Ricciardelli, F. and Vickery, J.B., 1999. "Tuned vibration absorbers with dry friction damping". *Earthquake Engineering & Structural Dynamics*, Vol. 28, No. 7, pp. 707–723.

Sallet, G., 2004. "Ordinary Differential Equations with Scilab WATS Lectures - Universitè de Saint-Louis". Page Web Prof. Gauthier Sallet. <http://www.iecl.univ-lorraine.fr/ Gauthier.Sallet/>.

Thomson, W.T. and Dahleh, M.D., 2005. *Theory of Vibration with Applications*. Pearson, 5th edition.

7. AUTHOR'S RESPONSIBILITIES

Authors are solely responsible for the information included in this work.